

for degenerate n -type material and assuming Keyes' calculated value for the electronic effect, then the expected electronic effect is -18.2×10^{-24} per incident electron/cm². From this and our observed length change obtained from Fig. 1, which was $\Delta L/L = -6.2 \times 10^{-24}$ per incident electron/cm², Eq. (1) then yields an atomic effect of $\Delta L/L = +12.0 \times 10^{-24}$ per incident electron/cm². By using the electron removal rate $dn/d\Phi = -13$ and the fact that each vacancy-interstitial pair formed is a double acceptor, the change in length per vacancy-interstitial pair is calculated to be $\Delta L/L = +1.85 \times 10^{-24}$ per defect pair/cm³. This implies a fractional atomic-volume change per vacancy-interstitial pair $(f_v + f_i) = +0.25$.

There are several factors which contribute to the uncertainty of the above calculations. Keyes' treatment compared the presence of electrons in the conduction band with their complete absence from the crystal, whereas in our case, electrons removed from the conduction band by the irradiation are trapped on tightly bound acceptor levels in the forbidden gap, which may quite plausibly not cause as large an effect. More work needs to be done concerning the dependence of the electronic effect upon the energy levels of the traps involved. Other factors are the rather large experimental uncertainties in the values of the deformation-potential constants needed in Keyes' cal-

culatation and the present uncertainty in the electron removal rate for degenerate material.

Even considering these uncertainties, it appears that the atomic effect is causing an expansion, but the magnitude of the contraction due to the electronic effect is larger, so that the observed contraction represents the difference between the two effects. It is hoped that our subsequent measurements will enable us to separate the two effects, and therefore allow us to determine both the electronic effect and the atomic effect experimentally.

The authors wish to express their gratitude to J. W. MacKay for his interest in this work and his many helpful discussions and suggestions, and to S. Rodriguez for stimulating discussions concerning the electronic effect.

*Work supported by Advanced Research Projects Agency and the National Science Foundation.

¹G. K. White, *Cryogenics* **1**, 151 (1961).

²E. E. Klontz and J. W. MacKay, *J. Phys. Soc. Japan* **18**, Suppl. 3, 216 (1963).

³M. P. Singh and J. W. MacKay, *Bull. Am. Phys. Soc.* **9**, 542 (1964).

⁴F. L. Vook and R. W. Balluffi, *Phys. Rev.* **113**, 62 (1959).

⁵M. C. Wittels, *J. Appl. Phys.* **28**, 921 (1957).

⁶F. L. Vook, *Phys. Rev.* **125**, 855 (1962).

⁷R. W. Keyes, *IBM J. Res. Develop.* **5**, 266 (1961).

⁸T. Figielski, *Physica Status Solidi* **1**, 306 (1961).

⁹T. A. Callcott and J. W. MacKay, to be published.

DOUBLE-QUANTUM PHOTOELECTRIC EMISSION FROM SODIUM METAL*

M. C. Teich,[†] J. M. Schroerer, and G. J. Wolga

Cornell University, Ithaca, New York

(Received 23 October 1964)

Theoretical calculations for the two-photon surface photoelectric effect in a metal have been given by Smith¹ and others.²⁻⁴ The theoretically predicted double-quantum photocurrent is proportional to the square of the incident radiation power and inversely proportional to the area irradiated.¹ Sonnenberg, Heffner, and Spicer⁵ have recently reported on the two-quantum photoelectric effect from a semiconductor in which the volume photoelectric effect predominates, giving rise to relatively large currents. We would like to report the first observation of double-quantum surface photoelectric emission from a metal. Two-photon photoelectric current was obtained from a sodium surface of work function 1.95 eV when

irradiated by photons of energy 1.48 eV from a GaAs laser.

The experimental apparatus is shown in the block diagram of Fig. 1. The radiation source was a pulsed GaAs semiconductor injection laser operated at 77°K and emitting a peak power of 400 mW at 8400 Å. A translation stage supporting a lens permitted the laser radiation to be focused onto a vapor-deposited sodium surface from which double-quantum photoemission was to be observed. This surface acted as a cathode for a specially constructed electron multiplier with a gain of 50 000. The amplified current was passed through a 1-MΩ load resistor followed by a low-noise preamplifier and a lock-in amplifier. Phase-sensi-

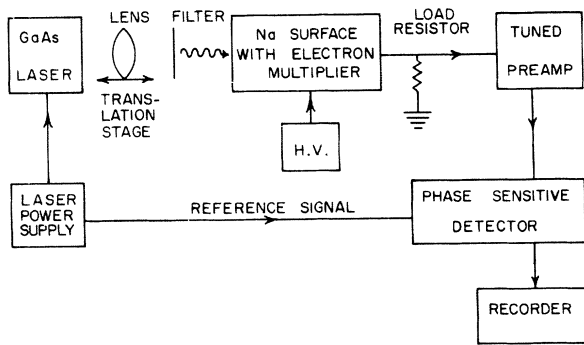


FIG. 1. Block diagram of apparatus.

tive detection was performed at 2.2 kc/sec which is the fundamental frequency of the pulse-modulated laser. The reference signal was obtained directly from the pulsed power supply driving the laser.

Filters calibrated at 8400 Å on a Cary spectrophotometer were inserted into the beam to provide known decrements of light power. Output voltage measurements were then recorded for each power level. The results of a typical run are shown in Fig. 2, where the photoelectric current has been plotted against the peak radiation power incident on the Na surface. The resulting experimental data may be fitted quite well by the curve A + B, obtained by adding line A of slope 1 to line B of slope 2. Line A shows a linear dependence of photoelectric current on light power and represents the single-quantum photoelectric contribution from the Fermi tail, while line B shows a quadratic dependence of photoelectric current on light power representing the double-quantum photo-current.

It is seen that the experimental points near the maximum values of incident power fall very close to line B, indicating that the total current in this region arises almost exclusively from two-quantum transitions. The admixture of single-quantum current at maximum incident power is seen to be less than 7%. At a peak radiation power of 400 mW, corresponding to 1.7×10^{18} photons/sec, the fundamental component of the two-quantum photoelectric current is 9×10^{-16} ampere. The knee of the curve, where the contribution of double- and single-quantum currents are equal, occurs at 6×10^{-18} ampere. This current corresponds to approximately 40 electrons/sec. Below this point, and down to the lowest current value measured (2×10^{-18} ampere corresponding to

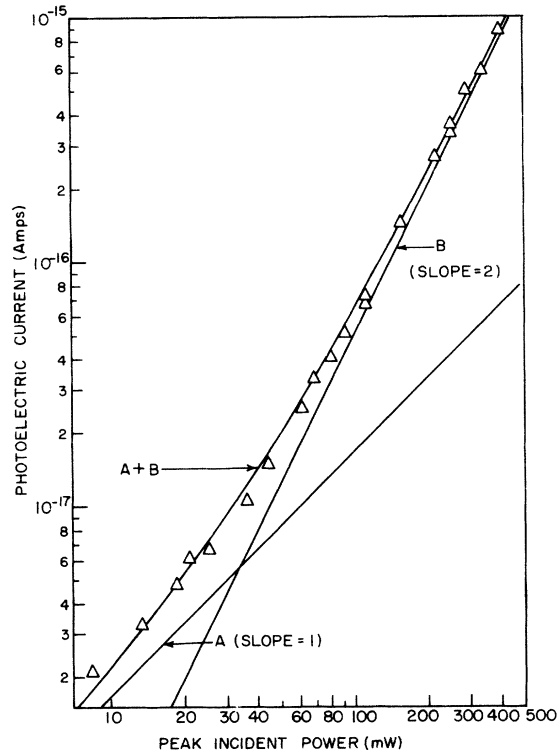


FIG. 2. Photoelectric current vs peak radiation power incident on the sodium surface for a typical run. At high powers, the current is seen to approach the line of slope 2, corresponding to double-quantum photoemission. As the power is reduced, the admixture of single-quantum photoelectrons from the Fermi tail increases, causing the current to approach the limit of slope 1.

12 electrons/sec), the curve showed a power dependence which was predominantly that of single-quantum emission.

Integration times of 3 and 10 sec were used in the upper and lower regions of current, respectively. In addition, visual integration of the recorder traces was performed. For the lower current levels, this integration time was sometimes as long as several minutes. A signal-to-noise ratio of approximately 3 was observed at 2×10^{-18} ampere prior to visual integration.

The noise-in-signal contribution to the signal-to-noise ratio, which arises from the statistics of the photoelectric emission, is given by $S/N = (i/2e\Delta F)^{1/2}$ where i is the average photoelectric signal current, $e = 1.6 \times 10^{-19}$ coulomb, and ΔF is the bandwidth of the final filter. The observed S/N obeyed this relation quite well, especially at current levels above 10^{-17} ampere where the S/N ranged from 10

to 100.

From the slope of line A, and the known radiation power content at the fundamental frequency, the yield $Y(T, \lambda)$ may be calculated:

$$Y(300^\circ\text{K}, 8400 \text{ \AA}) = 1.7 \times 10^{-15} \text{ A/W.}$$

Using this value of the photoelectric yield in a modification of the Fowler-DuBridge⁶ yield equation which is suitable for a photon energy approximately one-half the work function, we determined the work function to be 1.95 ± 0.02 eV. This is in excellent agreement with the value obtained independently from a Fowler plot which was 1.9 ± 0.1 eV for photons below 2.3 eV. At photon energies corresponding to $2h\nu = 2.96$ eV, however, the Fowler plot yielded a work function of 2.3 ± 0.1 eV. This latter value is therefore more appropriate for calculating the two-quantum current.

The average temperature change induced in a thermocouple by the focused laser beam was

measured to be 2°C . This permitted us to estimate a temperature rise of $<10^\circ\text{C}$ at the peak of the laser pulse, corresponding to a maximum thermionic emission current below 10^{-23} ampere. That thermionic emission was indeed not observable is borne out by the quadratic dependence of current over a large range of incident power.

Another possible cause of photoelectric emission was the second-harmonic generation of blue light (4200 \AA) in the laser itself. By measuring the yield $Y(T, \lambda)$ with and without a blue-attenuating filter in the laser beam, it was ascertained that the blue-light contribution to the photoelectric current was negligible. The peak second-harmonic power generated in the laser was found to be $<5 \times 10^{-12}$ watt for a power output of 0.4 watt at 8400 \AA.

Our result for the two-quantum photoelectric current may be compared with Smith's¹ theoretical calculation for a Sommerfeld metal. Use has been made of Bower's² corrected version of Eq. (51) in Smith's paper,

$$R(\beta_x) = \frac{\beta_x^2 (\beta_x^2 + 2\omega - W_a)^{1/2}}{4\omega - W_a + 2\beta_x^2 + 2[(2\omega + \beta_x^2)(2\omega - W_a + \beta_x^2)]^{1/2}} \\ \times \left\{ \frac{1}{2}W_a + \omega + 2[(\omega + \beta_x^2)(2\omega + \beta_x^2)]^{1/2} + 2[(W_a - \beta_x^2)(W_a - \omega - \beta_x^2)]^{1/2} \right\},$$

where the symbols are defined by Smith. The double-quantum current is evaluated using a photon energy of 1.48 eV, a work function of 2.3 eV, a Fermi level of 3.1 eV, and a fundamental Fourier component of the square of the laser intensity wave form equal to 0.1. The predicted two-quantum photoelectric current I is then

$$I = 9.7 \times 10^{-24} P^2/A \text{ ampere,}$$

where P represents the power incident on the Na surface and A is the area of the focused laser beam in mks units. Qualitative verification for an inverse area dependence is obtained from the large rise in output current when the lens is adjusted to image the laser emitting region on the sodium surface. The quadratic dependence of I on P has been amply demonstrated experimentally in Fig. 2. The focused laser spot on the sodium surface has been estimated to have an area of $5 \times 10^{-9} \text{ m}^2$. Inserting this area and an incident radiation power of

400 mW into this formula, we find

$$I_{\text{theor}}(400 \text{ mW}) = 3 \times 10^{-16} \text{ ampere.}$$

This may be compared with the experimental value from Fig. 2 at the same power:

$$I_{\text{expt}}(400 \text{ mW}) = 9 \times 10^{-16} \text{ ampere.}$$

An absolute comparison may not be made between the experimental and theoretical currents, however, because of experimental uncertainty in the gain of our system and the size of the focused spot on the sodium surface.

We are very grateful to A. L. McWhorter and T. M. Quist of Massachusetts Institute of Technology Lincoln Laboratory for making available to us the semiconductor injection lasers used in our experiments. We would also like to thank R. O. Carlson and T. J. Soltys of the General Electric Research Laboratory for providing us with laser diodes.

*This study was supported by the Advanced Research Projects Agency through the Materials Science Center at Cornell University.

†James Clerk Maxwell Fellow at Cornell University.

¹R. L. Smith, Phys. Rev. 128, 2225 (1962).

²H. C. Bowers, thesis, Cornell University, February 1964 (unpublished).

³I. Adawi, Phys. Rev. 134, A788 (1964).

⁴P. Bloch, J. Appl. Phys. 35, 2052 (1964).

⁵H. Sonnenberg, H. Heffner, and W. Spicer, Appl. Phys. Letters 5, 95 (1964).

⁶R. J. Maurer, Handbook of Physics, edited by E. U. Condon and Hugh Odishaw (McGraw-Hill Book Company, Inc., New York, 1958), Chap. 8.

PHONON-PUMPED SPIN-WAVE INSTABILITIES

H. Matthews

Bell Telephone Laboratories, Murray Hill, New Jersey

and

F. R. Morgenthaler*

Department of Electrical Engineering and Center for Materials Science and Engineering,
Massachusetts Institute of Technology, Cambridge, Massachusetts

(Received 12 October 1964)

We report here some theoretical results on the parametric excitation of spin waves by an elastic wave, together with experimental observations consistent with these results.

A phonon traveling in a magnetically saturated ferromagnet generates an effective magnetic field that can parametrically couple to spin waves. This field has the phonon momentum and, hence, spin-wave excitation by a traveling-wave pump is possible. The effective field may, in general, have components that are both transverse and parallel to the dc magnetic field. The former lead to modified Suhl instabilities,¹ the latter to modified "parallel pump" instabilities.^{2,3}

We restrict ourselves here to a discussion of the instabilities excited by a longitudinal phonon of frequency ω_p , and elastic displacement

$$\vec{\rho} = \vec{i}_z \rho_0 \cos(\omega_p t - \vec{k}_p \cdot \vec{r}), \quad (1)$$

whose wave vector, $\vec{k}_p = \vec{i}_z k_p$, is parallel to the dc magnetic field.

We consider the first-order excitation of spin-wave pairs when the pump phonon travels in a cubic crystal of ellipsoidal shape magnetically saturated along a principal axis taken, for simplicity, parallel to a $\langle 100 \rangle$ crystal axis. The classical equations of motion governing spin-wave propagation follow from

$$\partial \vec{M} / \partial t = \gamma \vec{M} \times \vec{H}, \quad (2)$$

in which γ denotes the gyromagnetic ratio (negative). The magnetization is assumed to be composed of a spin-wave pair, \vec{m}_1 and \vec{m}_2 , so that

$\vec{M} = \vec{m}_1 + \vec{m}_2 + \vec{i}_z M_s$. The i th spin wave, whose wave vector is

$$\vec{k}_i = k_i \sin \Psi_i (\vec{i}_x \cos \xi_i + \vec{i}_y \sin \xi_i) + k_i \cos \Psi_i \vec{i}_z, \quad (3)$$

is represented by

$$\begin{aligned} \vec{m}_i = & \vec{i}_x m_{ix} \cos(\omega_i t - \vec{k}_i \cdot \vec{r} + \varphi_{ix}) \\ & + \vec{i}_y m_{iy} \sin(\omega_i t - \vec{k}_i \cdot \vec{r} + \varphi_{iy}), \end{aligned} \quad (4)$$

and M_s denotes the saturation magnetization. To account for the Zeeman, demagnetizing, exchange, dipolar, and magnetic anisotropy energies and to include loss, $\vec{H} = \vec{h}_1 + \vec{h}_2 + \vec{i}_z H_z$, where

$$\vec{h}_i = -\lambda k_i^2 \vec{m}_i - 4\pi \frac{\vec{k}_i (\vec{k}_i \cdot \vec{m}_i)}{k_i^2} + \frac{\Delta H_i}{2M_s} (\vec{i}_x m_{iy} - \vec{i}_y m_{ix}), \quad (5)$$

and

$$H_z = H_0 - 4\pi N_z M_s + 2K_1 / M_s. \quad (6)$$

In these expressions H_0 denotes the external applied field, N_z the corresponding demagnetizing factor, λ the exchange constant, K_1 the magnetic anisotropy constant, ΔH_i the full linewidth of the i th spin wave.

The magnetoelastic energy is given by

$$U = (b_1 / M_s^2) M_z^2 \partial \rho_z / \partial z. \quad (7)$$

Together with Eq. (1) this leads to the effec-